Carbonatation and Decarbonatation Kinetics in the La2O3-La2O2CO3 System under CO2 Gas Flows

Bahcine Bakiz, Frédéric Guinneton, Madjid Arab, Abdeljalil Benlhachemi, Sylvie Villain, Pierre Satre, Jean-Raymond Gavarri

Hindawi Publishing Corporation
Advances in Materials Science and Engineering
Volume 2010, Article ID 360597, 6 pages
doi:10.1155/2010/360597

Research Article

Carbonatation and Decarbonatation Kinetics in the La_2O_3-$La_2O_2CO_3$ System under CO_2 Gas Flows

Bahcine Bakiz,[1,2] Frédéric Guinneton,[1] Madjid Arab,[1] Abdeljalil Benlhachemi,[2] Sylvie Villain,[1] Pierre Satre,[1] and Jean-Raymond Gavarri[1]

[1] *Institut Matériaux Microélectronique & Nanosciences de Provence, UMR CNRS 6242, Université du SUD Toulon-Var, BP 20132, 83957 La Garde Cedex, France*
[2] *Laboratoire Matériaux et Environnement, Faculté des Sciences, Université Ibn Zohr, BP 8106, 80000 Agadir, Morocco*

Correspondence should be addressed to Jean-Raymond Gavarri, gavarri.jr@univ-tln.fr

Received 26 May 2010; Revised 2 July 2010; Accepted 5 August 2010

Academic Editor: Sridhar Komarneni

The carbonatation of La_2O_3 oxide and the decarbonatation of lanthanum carbonate phase $La_2O_2CO_3$ are investigated using thermal and thermogravimetry analyses under CO_2 gas flow. The initial phase La_2O_3 is first elaborated from pyrolysis of a $LaOHCO_3$ precursor. Then, thermal and thermogravimetry analyses are carried out under CO_2 flow, as temperature increases then decreases. The carbonatation kinetics of La_2O_3 is determined at three fixed temperatures. Electrical impedance spectroscopy is performed to determine the electrical responses associated with ionic mobilities and phase changes, in the temperature range 25 to 900°C. The electrical conduction during heating under CO_2 gas flow should be linked to two regimes of ionic conduction of the carbonate ions. From these electrical measurements, the ionic mobility of carbonate ions CO_3^{2-} is found to be close to 0.003 $\cdot 10^{-4}$ $cm^2\ s^{-1}\ V^{-1}$ at 750°C for the monoclinic $La_2O_2CO_3$ phase.

1. Introduction

The lanthanum-based system La_2O_3-CO_2-H_2O is characterized by successive phases $LaOHCO_3$, $La_2O_2CO_3$, and La_2O_3, stable in various temperature ranges [1–9], depending on the partial pressures of CO_2 and H_2O [10–15]. It has been established that the decomposition of the hydroxycarbonate $LaOHCO_3$ under air generally gives the $La_2O_2CO_3$ dioxycarbonate phase [6]. However, this last phase exists under three polymorphic structural varieties with tetragonal, hexagonal, and monoclinic crystal lattices [16–19]. The carbonatation of La_2O_3 under pure CO_2 generally gives the main $La_2O_2CO_3$ phase; however, the obtained system can be complex, with presence of several polymorphic structures depending on the experimental synthesis conditions [10, 18, 20]. In their work concerning the TG analysis of the $La_2O_2CO_3$ phase under CO_2 gas, the authors of [2] showed that a small amount of $La_2O(CO_3)_2$ was probably formed as an additional phase. This phase was also studied by authors of [21].

In room conditions, the lanthanum oxide is highly sensitive to environmental water. In a previous study [22], we have established correlations between the thermal decomposition and the electrical responses of compacted pellets of this $LaOHCO_3$ phase, subjected to pyrolysis under air: we have shown that strong variations in conductances accompanied these phase changes. We have also established that these $LaOHCO_3$, $La_2O_2CO_3$, and La_2O_3 phases have the capacity to convert carbon monoxide into CO_2 at relatively low temperature: at 200–300°C, the L phase is a good catalyst converting CO into CO_2, while it might be sensitive to CO_2 only above 500°C.

In the present study, we focus our attention on phase changes during carbonatation and decarbonatation processes, respectively, of the La_2O_3 phase and of the $La_2O_2CO_3$ phase. The main objective of this approach should reside in connecting the weight variations due to these phase transformations with electrical responses, in order to appreciate their potential efficiency in gas sensing devices. These correlations between mass losses and electrical responses are

not known, and they could deliver interesting information on the electrical sensitivity of such systems.

2. Experimental Details

The $LaOHCO_3$ hydroxycarbonate was first prepared via a specific route [22, 23] based on a thermal treatment at 80°C of three aqueous solutions of $La(NO_3)_3 \cdot 6H_2O$, urea $CO(NH_2)_2$, and polyvinyl-pyrrolydine (PVP) polymer. The La_2O_3 oxide was obtained by pyrolysis of this $LaOHCO_3$ precursor.

The various chemical steps can be summarized as follows:

(i) First initial decomposition processes under air as temperature increases (25–1200°C):

$$LaOHCO_3 \longrightarrow La_2O_2CO_3\ [1] + H_2O + CO_2, \quad (1)$$

$$La_2O_2CO_3\ [1] \longrightarrow La_2O_3\ [1] + CO_2. \quad (1')$$

(ii) Carbonatation and decarbonatation under pure CO_2 as temperature increases (25–1200°C):

$$La_2O_3\ [1] + CO_2 \longrightarrow La_2O_2CO_3\ [2], \quad (2)$$

$$La_2O_2CO_3\ [2] + CO_2 \longrightarrow La_2O_3\ [2] + 2\ CO_2. \quad (2')$$

(iii) Recarbonatation under pure CO_2 as temperature decreases (1200 to 25°C):

$$La_2O_3\ [2] + CO_2 \longrightarrow La_2O_2CO_3\ [3]. \quad (3)$$

In the previous equations, in bracket [1 to 3] we have designated phases obtained after a transformation process (decomposition, carbonatation, and decarbonatation). Theses phases have not the same characteristics (various morphologies and specific surfaces).

The polycrystalline samples were systematically analyzed by X-ray diffraction, using a D5000 Siemens-Bruker diffractometer, equipped with a copper X-ray source (wavelength $\lambda = 1.54\,10^{-10}$ m), and with a monochromator eliminating Kβ radiation. The experiments were carried out using classical $\theta - 2\theta$ configuration.

Thermal and Thermogravimetric analyses (DTA-TG) were carried out using SETARAM DSC 92 equipment, with a thermal rate of 10°C/minute, under CO_2 pure gas (rate of flow of 33 $cm^3 \cdot s^{-1}$).

Electrical measurements under CO_2 gas flow were performed using a Solartron electrical impedance spectrometer working with a maximal tension of 1 V, in the frequency range 100 to 10^7 Hz. A reactive homemade cell was used to perform experiments under various gas flows (air, CO_2) at various temperatures ranging between 25 and 900°C. The spectrometer delivers Nyquist representations of the resulting impedances recorded at fixed temperatures: the resistance value is classically obtained by extrapolation of the experimental Nyquist circles, and using electrical equivalent circuits (parallel *R-C* circuits) generated by the software. We have selected specific electrical circuits with a resistance (R) parallel to a constant phase element CPE $= (jC^*\omega)^n$ where the exponent n is comprised between 1 and 0, and C^* is a term similar to a capacitance for $n = 1$ (the unit of C^* depends on n).

To obtain electrical analyses of sample surfaces reacting with gas flows, the powder samples were first compacted under a pressure of 5 kbar in a cylindrical cell. Then, the obtained cylindrical pellet was cut in form of a rectangular plate, with platinum electrodes fixed on two parallel faces (dimensions 2.3 × 8 mm). The distance between the electrodes is 9 mm. This configuration (adapted to the reactive cell) allows a determination of the electrical properties of a significant material surface exposed to gas action. In a later step, these results might be used to test a hypothetical gas sensor sensitive to CO_2.

3. Results

3.1. Carbonatation-Decarbonatation Processes

3.1.1. Heating Process under CO_2 Flow. The La_2O_3 sample, initially obtained from thermal decomposition of $LaOHCO_3$, has been subjected to thermal and thermogravimetry analyses under CO_2 gas flow, with temperature increasing from 25 to 1200°C. The resulting TG-DTA curves are reported on Figure 1. A strong exothermic DTA peak is observed at 525°C: it is related to the carbonatation of La_2O_3 with formation of the $La_2O_2CO_3$ phase. Then, at 960°C, we observe an endothermic feature corresponding with the decomposition of the carbonate phase. Above 980°C the La_2O_3 phase stabilizes. A small endothermic feature is observed at 375°C: it might be associated with a partial dehydration of the sample due to the high sensitivity to environmental water of La_2O_3. The progressive mass evolution observed in the TG curve of Figure 1, as temperature increases, is directly associated with the classical buoyancy. A similar effect will be observed during the cooling process.

3.1.2. Cooling Experiments under CO_2 Flow. Using cooling experiments, we have analyzed the carbonatation of La_2O_3 from 1200°C to 25°C. The results are represented on Figure 2. The formation of $La_2O_2CO_3$ starts from 820°C and is maximum at 750°C. The exothermic peak associated with the crystallization of $La_2O_2CO_3$ carbonate is observed at 790°C. This temperature of carbonatation is strongly different from the one obtained during the heating process.

At each step involving a stabilized phase, we have carried out X-ray diffraction analyses to identify the obtained phases. We have confirmed that, in the case of thermal decomposition under air of $LaOHCO_3$ phase, two different tetragonal and hexagonal $La_2O_2CO_3$ structures are simultaneously observed. In the case of carbonatation of the La_2O_3 phase in the temperature range 500 to 700°C, we observe the formation of the $La_2O_2CO_3$ phase. The $La_2O(CO_3)_2$ phase was not observed in our experiments. This fact was previously reported by other authors [10, 18]. On Figure 3, we have reported the X-ray diffraction pattern characteristic

Table 1: Parameters extracted from Avrami's model: k_1 and k_2 kinetics parameters and p_1 and p_2 exponents, respectively, associated with the fast and slow regimes (1st and 2nd periods).

	1st period			2nd period		
T (°C)	Time range (min)	k_1	p_1	Time range (min)	k_2	p_2
450	45 → 112	$1.5\,10^{-7}$	3.3	167 → 320	0.02	0.9
480	6 → 17	$1.4\,10^{-5}$	3.9	30 → 90	0.54	0.3
500	3 → 7	$1.2\,10^{-3}$	3.4	30 → 90	1.10	0.2
	Activation energies E_1 (k_1)	7.6 (eV)		Activation energies E_2 (k_2)	2.8 (eV)	

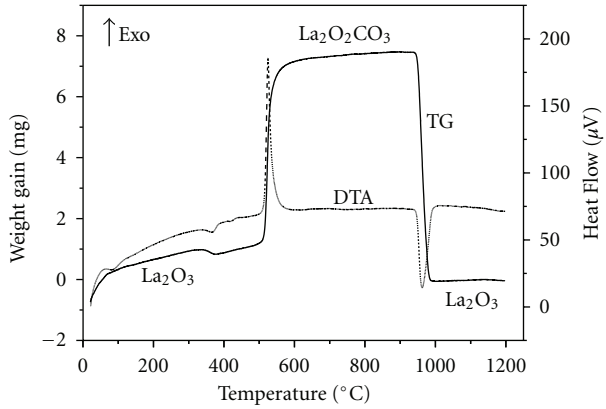

Figure 1: Weight gain associated with carbonatation of La_2O_3 (first step): exothermic peak at 520°C linked with weight gain due to formation of the monoclinic $La_2O_2CO_3$ phase; endothermic peak due to decarbonatation of $La_2O_2CO_3$ phase and formation of final La_2O_3 (second step).

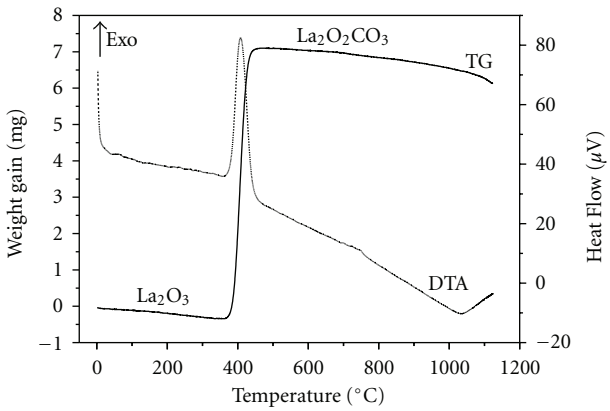

Figure 2: Evolution of La_2O_3 weight during cooling process, under CO_2 flow: formation of $La_2O_2CO_3$ phase (exothermic peak) then relative stabilization of this phase as temperature decreases.

of the monoclinic $La_2O_2CO_3$ phase heated at 520°C under CO_2 flow, during 3 hours. The refined cell parameters are $a = 0.4073 \pm 0.0003$ nm; $b = 1.3503 \pm 0.0008$ nm; $c = 0.4079 \pm 0.0005$ nm; $\beta = 90.89°$. In the pattern, a weak trace of the hexagonal phase (noted as $*$) is observed.

3.2. Kinetics Study of Carbonatation of La_2O_3 at Fixed Temperatures. We have performed a weight analysis of the La_2O_3 powder, obtained from the thermal decomposition of the initial $LaOHCO_3$ phase, under CO_2 gas flow at three constant temperatures. The CO_2 gas flow rate was $33\,cm^3 \cdot s^{-1}$. In the SETARAM equipment, a fast temperature increase is first applied to the sample, and then, the temperatures are successively fixed to 450, 480, and 500°C. The three initial masses of La_2O_3 are successively (at $T = 450$, 480, and 500°C) $m_0 = 74.36$ mg, 70.73 mg, and 39.26 mg. The data evolutions have been interpreted in terms of an elemental Avrami's model [24] (using a single mechanism approach):

$$\Delta m = \Delta m_0\left[1 - \exp(-k \cdot t^p)\right], \tag{4}$$

(i) t is the reaction time;

(ii) Δm_0 is the limit mass of CO_2 involved in the carbonate formation $La_2O_2CO_3$ from a mass m_0 of La_2O_3;

(iii) Δm is the CO_2 mass having reacted with La_2O_3 at the time t;

(iv) k is a kinetics parameter depending of temperature;

(v) p is the exponent characteristic of the reaction mechanism ($p > 2$ for complex mechanisms, $p < 1$, for example, for mechanisms involving diffusion barriers).

To test the degree of validity of this Avrami's model, we have reported the function Y versus $\ln(t)$ on Figure 4:

$$Y = \ln\left[-\frac{\ln(\Delta m_0 - \Delta m)}{\Delta m_0}\right] = \ln(k) + p\ln(t). \tag{5}$$

For a single crystal growth mechanism, the variation of Y versus $\ln(t)$ should have been linear. Presently, the representation of Figure 4 is not linear: this should be mainly due to the existence of at least two different crystal growth mechanisms, with two periods of mass gain corresponding to two behaviors.

In Table 1, we have reported the values of the kinetics parameters k_1 and k_2 and exponents p_1 and p_2, corresponding with the two different behaviors in which a linear correlation might be observed. The parameters k_1, p_1 are relative to the first period depending on temperature, and the parameters k_2, p_2 are relative to the second period. The k_1 and k_2 are thermally activated with activation energies of, respectively, 7.6 and 2.8 eV. The p_1 exponent is quasi-constant, while the p_2 exponent is close to 1 at 450°C and becomes very weak at higher temperatures.

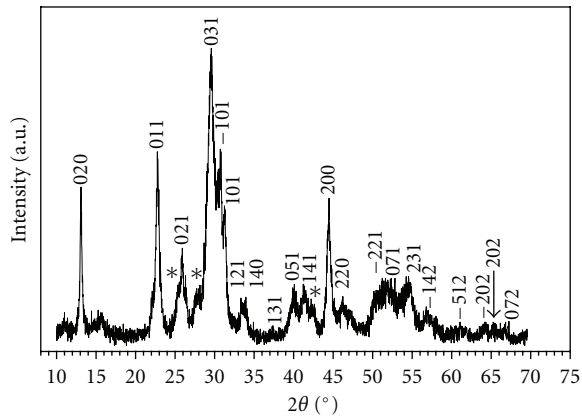

FIGURE 3: X-ray diffraction pattern of $La_2O_2CO_3$ (monoclinic) obtained by heating La_2O_3 at 520°C under CO_2 flow. Trace of hexagonal phase (noted ∗).

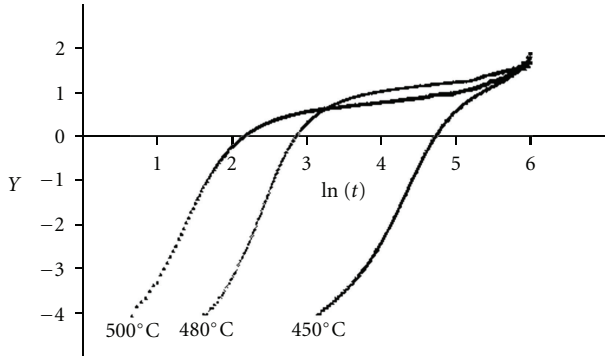

FIGURE 4: Test of Avrami's model validity: the representation of $Y = \ln[-\ln(\Delta m_0 - \Delta m)/\Delta m_0]$ versus $\ln(t)$ (t in mn) shows that two main types of behaviors can be observed as time increases.

The first growth regime should be associated with a fast carbonatation of grain surfaces associated with complex diffusion mechanisms. During this period, a carbonate shell enveloping oxide grains probably should be formed. The second growth regime should be associated with reaction and diffusion in grain cores, with a decrease of the reaction rate due to the carbonate shell: the resulting slow diffusion regime could govern the global reaction speed.

3.3. Electrical Analyses under CO_2 Gas Flows. To correlate the phase modifications to electrical behaviors, we have analyzed compacted powder samples in the electrical cell. In this experiment, a rectangular compacted sample resulting from the total decomposition of the initial $LaOHCO_3$ sample has been subjected to a progressive heating, under pure CO_2 gas flow. Between 600 and 700°C, carbonatation occurs, thus involving a strong increase in conductance mainly due to the ionic mobility of CO_3^{2-} carbonate ions. Then, above 750°C decarbonation occurs, involving a decrease of conductance due to CO_3^{2-} carbonate ions elimination and formation of La_2O_3. This oxide should be formed at 950°C.

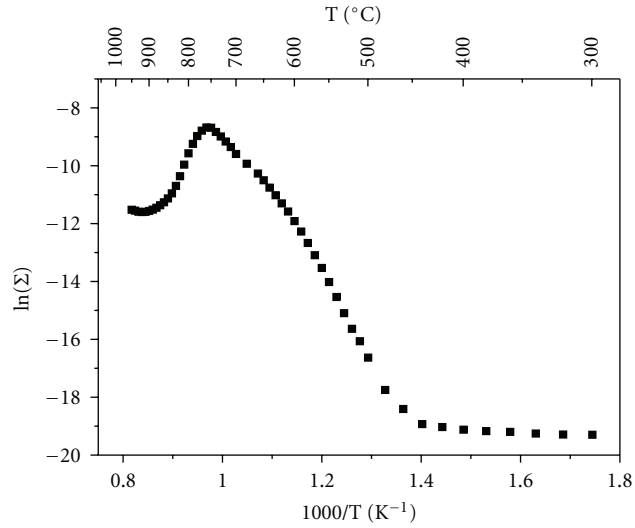

FIGURE 5: Evolution of $\ln(\Sigma)$ versus 10^3/T of initial La_2O_3 sample during its carbonatation and decarbonatation, in the temperature range 300 to 950°C, under a constant CO_2 gas flow: (a) starting step of carbonatation between 450 and 750°C with two conduction regimes; (b) decarbonatation step above 750°C.

On Figure 5, we have reported the $\ln(\Sigma)$ values versus temperature (total Σ values). We observe a strong decrease of $\ln(\Sigma)$ between 450°C and 750°C: the carbonatation of La_2O_3 should start from 450°C, with a first regime up to 600°C and a second regime up to 750°C. Two activation energies for the conduction behavior can be determined: 2.5 (first regime) and 1.4 eV (second regime). In this carbonatation domain, the ionic conduction plays a major role with mobile species CO_3^{2-}.

Above 750°C, we observe a strong decrease in the $\ln(\Sigma)$ values: in this temperature range, decarbonatation occurs in a continuous way, with the elimination of CO_3^{2-} ions. As La_2O_3 phase stabilizes, the resistance reaches a stabilized value.

Using the observed value $\Sigma = 1.7 \cdot 10^{-4}\,\Omega^{-1}$ at 750°C (on Figure 5: maximum value of Σ just before decomposition), and considering as negligible the conductance of La_2O_3 at the same temperature (close to 10^{-8} to $10^{-9}\,\Omega^{-1}$ at 750°C), we have evaluated an ionic conductance due to CO_3^{2-} ions to $\Delta\Sigma = 1.7 \cdot 10^{-4}\,\Omega^{-1}$. From this evaluation of $\Delta\Sigma$, we have determined the order of magnitude of the carbonate ion mobility $u(CO_3^{2-})$ at 750°C. Other values could be derived from the data obtained in the temperature range 450 to 700°C. The concentration of carbonate ions C_{ion} has been calculated from the effective density of the sample $\mu = 5.1\,\text{g}\cdot\text{cm}^{-3}$ (for a theoretical crystal density of 6.51 g.cm^{-3}) and using the sample volume $V = 0.1656\,\text{cm}^3$. A value of $C_{\text{ion}} = 0.0155\,\text{mol}\cdot\text{cm}^{-3}$ has been obtained. To determine the mobility, we have used the classical relations:

$$\Delta\Sigma = \sigma\frac{S}{L}, \qquad \sigma = Q \cdot C_{\text{ion}} \cdot u(\text{ion}), \tag{6}$$

where σ is the conductivity, S and L are the surface and separation distance of the two electrodes, and where

$Q = 193\,000\ \mathrm{C \cdot mol^{-1}}$. The relation giving the conductivity assumes an activity coefficient of 1: it only delivers an order of magnitude for the mobility.

We have obtained an order of magnitude of $u(CO_3^{2-}) = (0.003 \pm 0.001)\ 10^{-4}\ \mathrm{cm^2\ s^{-1}\ V^{-1}}$ for a carbonate ion moving at 750°C mainly along grain boundaries (or grain surfaces), and partly in the grain cores. This relatively high mobility can be associated with the activation energy of 1.4 eV (in the temperature range 600 to 750°C) as calculated above.

4. Discussion-Conclusions

The carbonatation kinetics of La_2O_3 has been determined at various temperatures. In the case of mass gain analyses, an elemental Avrami's approach has allowed determining a complex two-step mechanism of growth: (i) a fast surface carbonatation with carbonate shell formation and (ii) a diffusion mechanism in grain cores with slower kinetics. The electrical analyses argue in favor of two different conduction mechanisms: during carbonatation at increasing temperature, the first activation energy (2.5 eV) should be associated with ionic conduction at grain surfaces, and the second activation energy (1.4 eV) should due to an increasing contribution of the conduction in the bulk. Correlatively, it should be remarked that, in thermal analyses, the stability range is observed from 500 to 850°C, while in electrical analyses, this stability range is observed from 500 to 750°C. This can be explained by the two different heating kinetics conditions used in the two experiments.

Finally, we observe a relatively high ionic mobility mainly due to the CO_3^{2-} ions in $La_2O_2CO_3$ at 750°C. In our evaluation, we have neglected the ionic conduction of oxygen ions.

It should be concluded that these phase modifications associated with high ionic conduction might be used as electrical sensitive material to detect CO_2, provide temperatures that could be fixed close to 400–550°C (carbonatation of La_2O_3 phase) and 750°C to restore the initial La_2O_3 phase.

Acknowledgments

The authors gratefully acknowledge the Provence-Alpes-Côte d'Azur Regional Council, the General Council of Var, and the agglomeration community of Toulon Provence Mediterranean for their helpful financial supports. This paper was developed in the general framework of ARCUS CERES project (2008–2010).

References

[1] E. Béchade, I. Julien, T. Iwata et al., "Synthesis of lanthanum silicate oxyapatite materials as a solid oxide fuel cell electrolyte," *Journal of the European Ceramic Society*, vol. 28, no. 14, pp. 2717–2724, 2008.

[2] A. N. Shirsat, M. Ali, K. N. G. Kaimal, S. R. Bharadwaj, and D. Das, "Thermochemistry of $La_2O_2CO_3$ decomposition," *Thermochimica Acta*, vol. 399, no. 1-2, pp. 167–170, 2003.

[3] S. Valange, A. Beauchaud, J. Barrault, Z. Gabelica, M. Daturi, and F. Can, "Lanthanum oxides for the selective synthesis of phytosterol esters: correlation between catalytic and acid-base properties," *Journal of Catalysis*, vol. 251, no. 1, pp. 113–122, 2007.

[4] O. K. Nikol'skaya and L. N. Dem'yanets, "Hydrothermal crystallization in the systems $La_2(CO_3)_3 \cdot 6H_2O$-$CaCO_3$($BaCO_3$)-R-H_2O(R = Na_2, $CO_3K_2CO_3$, $NaHCO_3$, $KHCO_3$, NaCl, NH_4Cl, $CO(NH_2)_2$)," *Inorganic Materials*, vol. 41, no. 11, pp. 1206–1212, 2005.

[5] M. L. Panchula and M. Akinc, "Morphology of lanthanum carbonate particles prepared by homogeneous precipitation," *Journal of the European Ceramic Society*, vol. 16, no. 8, pp. 833–841, 1996.

[6] H. Wakita and S. Kinoshita, "A synthetic study of the solid solutions in the systems and $La_2(CH_3)_3 \cdot 8H_2O$-$Ce_2(CO_3)_3 \cdot 8H_2O$ and $La(OH)CO_3$-$Ce(OH)CO_3$," *Bulletin of the Chemical Society of Japan*, vol. 52, pp. 428–432, 1979.

[7] G. A. M. Hussein and H. M. Ismail, "Characterization of lanthanum oxide formed as a final decomposition product of lanthanum acetylacetonate: thermoanalytical, spectroscopic and microscopic studies," *Powder Technology*, vol. 84, no. 2, pp. 185–190, 1995.

[8] B. Bakiz, K. Ouzaouit, A. Benlhachemi, et al., "Multiphase lanthanum hydroxycarbonates and langasite ceramics for gas sensors," *Physical and Chemical News*, vol. 41, pp. 55–60, 2008.

[9] B. A. A. Balboul, A. M. El-Roudi, E. Samir, and A. G. Othman, "Non-isothermal studies of the decomposition course of lanthanum oxalate decahydrate," *Thermochimica Acta*, vol. 387, no. 2, pp. 109–114, 2002.

[10] T. J. Toops, A. B. Walters, and M. A. Vannice, "The effect of CO_2 and H_2O on the kinetics of NO reduction by CH_4 over a La_2O_3/γ-Al_2O_3 catalyst," *Journal of Catalysis*, vol. 214, no. 2, pp. 292–307, 2003.

[11] Y. Cui, H. Zhang, H. Xu, and W. Li, "The CO_2 reforming of CH_4 over Ni/La_2O_3/α-Al_2O_3 catalysts: the effect of La_2O_3 contents on the kinetic performance," *Applied Catalysis A*, vol. 331, no. 1, pp. 60–69, 2007.

[12] J. Gao, Z. Hou, J. Guo, Y. Zhu, and X. Zheng, "Catalytic conversion of methane and CO_2 to synthesis gas over a La_2O_3-modified SiO_2 supported Ni catalyst in fluidized-bed reactor," *Catalysis Today*, vol. 131, no. 1–4, pp. 278–284, 2008.

[13] T. Esaka and K. Motoike, "CO_2 absorption and desorption of Bi_2O_3-La_2O_3 powders prepared by mechanical synthesis," *Materials Research Bulletin*, vol. 39, no. 11, pp. 1581–1587, 2004.

[14] T. Esaka and K. Motoike, "Absorption and desorption of carbon dioxide in the rare earth oxide-doped Bi_2O_3 powder," *Journal of Alloys and Compounds*, vol. 408–412, pp. 480–483, 2006.

[15] H. Chen, H. Yu, F. Peng, H. Wang, J. Yang, and M. Pan, "Efficient and stable oxidative steam reforming of ethanol for hydrogen production: effect of in situ dispersion of Ir over Ir/La_2O_3," *Journal of Catalysis*, vol. 269, no. 2, pp. 281–290, 2010.

[16] A. Olafsen, A.-K. Larsson, H. Fjellvåg, and B. C. Hauback, "On the crystal structure of $Ln_2O_2CO_3$ II (Ln=La and Nd)," *Journal of Solid State Chemistry*, vol. 158, no. 1, pp. 14–24, 2001.

[17] K. Koyabu, T. Masui, S. Tamura, and N. Imanaka, "Synthesis of a new phosphor based on rare earth oxycarbonate," *Journal of Alloys and Compounds*, vol. 408–412, pp. 867–870, 2006.

[18] H. Chen, H. Yu, F. Peng, H. Wang, J. Yang, and M. Pan, "Efficient and stable oxidative steam reforming of ethanol for hydrogen production: effect of in situ dispersion of Ir over Ir/La_2O_3," *Journal of Catalysis*, vol. 269, no. 2, pp. 281–290, 2010.

[19] K. Efimov, M. Arnold, J. Martynczuk, and A. Feldhoff, "Crystalline intermediate phases in the sol-gel-based synthesis of $La_2NiO_{4+\delta}$," *Journal of the American Ceramic Society*, vol. 92, no. 4, pp. 876–880, 2009.

[20] T. J. Toops, A. B. Walters, and M. A. Vannice, "The effect of CO_2, H_2O and SO_2 on the kinetics of NO reduction by CH_4 over La_2O_3," *Applied Catalysis B*, vol. 38, no. 3, pp. 183–199, 2002.

[21] S. R. Dharwadkar, M. S. Kumbhar, M. S. Chandrasekharaiah, and M. D. Karkhanavala, "Thermal decomposition of lanthanum formate," *Journal of Inorganic and Nuclear Chemistry*, vol. 42, no. 11, pp. 1621–1625, 1980.

[22] B. Bakiz, F. Guinneton, M. Arab, S. Villain, A. Benlhachemi, and J. R. Gavarri, "Temperature dependent electrical properties and catalytic activities of La_2O_3-CO_2-H_2O phase system," *Advances in Materials Science and Engineering*, vol. 2009, Article ID 612130, 4 pages, 2009.

[23] B. Bakiz, F. Guinneton, J.-P. Dallas, S. Villain, and J.-R. Gavarri, "From cerium oxycarbonate to nanostructured ceria: relations between synthesis, thermal process and morphologies," *Journal of Crystal Growth*, vol. 310, no. 12, pp. 3055–3061, 2008.

[24] E. C. N. Lopes, F. S. C. Dos Anjos, E. F. S. Vieira, and A. R. Cestari, "An alternative Avrami equation to evaluate kinetic parameters of the interaction of Hg(II) with thin chitosan membranes," *Journal of Colloid and Interface Science*, vol. 263, no. 2, pp. 542–547, 2003.